Phototoxic effects of PAH and UVA exposure on molecular responses and developmental success in coral larvae

Sebastian Overmans[a,*], Mikaela Nordborg[b,c], Rubén Díaz-Rúa[a], Diane L. Brinkman[b], Andrew P. Negri[b], Susana Agustí[a]

[a] *Red Sea Research Center (RSRC), King Abdullah University of Science and Technology (KAUST), Thuwal 23955, Saudi Arabia*
[b] *Australian Institute of Marine Science (AIMS), Townsville 4810, Queensland, Australia*
[c] *James Cook University (JCU), Townsville, Queensland 4811, Australia*

ABSTRACT

Exposure to polycyclic aromatic carbons (PAHs) poses a growing risk to coral reefs due to increasing shipping and petroleum extraction in tropical waters. Damaging effects of specific PAHs can be further enhanced by the presence of ultraviolet radiation, known as phototoxicity. We tested phototoxic effects of the PAHs anthracene and phenanthrene on larvae of the scleractinian coral *Acropora tenuis* in the presence and absence of UVA (320–400 nm). Activity of superoxide dismutase (SOD) enzyme was reduced by anthracene while phenanthrene and UVA exposure did not have any effect. Gene expression of *MnSod* remained constant across all treatments. The genes *Catalase*, *Hsp70* and *Hsp90* showed increased expression levels in larvae exposed to anthracene, but not phenanthrene. Gene expression of *p53* was upregulated in the presence of UVA, but downregulated when exposed to PAHs. The influence on stress-related biochemical pathways and gene expresson in *A. tenuis* larvae was considerably greater for anthracene than phenanthrene, and UVA-induced phototoxicity was only evident for anthracene. The combined effects of UVA and PAH exposure on larval survival and metamorphosis paralleled the sub-lethal stress responses, clearly highlighting the interaction of UVA on anthracene toxicity and ultimately the coral's development.

1. Introduction

Scleractinian corals are the foundation organisms of tropical coral reefs, providing the physical structures and habitats that support the world's most diverse and complex communities. The health of coral reefs depends on the ability of corals to cope with biotic and abiotic stressors, and widespread damage to these, often sensitive, foundation organisms could lead to a collapse of the ecosystem (Hughes et al., 2003; Pandolfi et al., 2003). An estimated 20% of reefs worldwide have been lost as a consequence of natural and anthropogenic disturbances, and a further 15% are in a critical state and likely to be lost within the next few decades (Hughes et al., 2010). The Great Barrier Reef (GBR) is the world's best legislatively-protected extensive reef system, and here coral cover declined by over 50% between the years 1985 and 2012 (De'ath et al., 2012). Since then, successive widespread thermal bleaching events have resulted in further mass mortality in the GBR (Hughes et al., 2017).

Corals worldwide are under increasing environmental pressure with many threats identified including global changes such as ocean warming, acidification, eutrophication, hydrocarbon pollution and increased human activities in coastal areas (Pandolfi et al., 2011), contributing to cumulative detrimental pressure on reefs (Hughes et al., 2010). Reducing local stressors, including pollution, is considered an important strategy to slow the decline of coral reefs due to global pressures (De'ath et al., 2012).

Oil and gas extraction frequently occurs near coral reefs throughout South East Asia, in the Middle East, the Caribbean and off northwestern Australia, and shipping traffic continuously increases in proximity to reefs, including the GBR (PGM-Environment, 2012; Wilkinson, 1999). These activities contribute to a low likelihood but potentially catastrophic risk from spills to tropical reef ecosystems. Components of oil, particularly the polycyclic aromatic hydrocarbons (PAHs) are toxic to corals and other reef organisms (Negri et al., 2016; Teal and Howarth, 1984; Turner and Renegar, 2017). While PAHs can have a substantial effect on the survival of existing coral reef communities (Dodge et al., 1984; Rinkevich and Loya, 1977; Rinkevich and Loya, 1979), sub-lethal concentrations of PAHs can have a severe impact on early life stages of coral. At those concentrations, larval health and settlement can be

---

diminished, which in turn slows down recruitment and recovery of reefs following damage due to a spill (Hartmann et al., 2015; Villanueva et al., 2011). Indeed spills such as the uncontrolled 10,000 m³ Galeta release in Panama in 1986 caused impacts on coral communities lasting decades at least partially due to impaired larval recruitment (Guzman et al., 1994).

A critical phenomenon relevant to organisms at risk of exposure to oil and PAHs is phototoxicity, where the damaging effects of some PAHs can increase in the presence of ultraviolet radiation (UVR) (Willis and Oris, 2014). Phototoxicity is of particular importance for tropical reef ecosystems where the penetration and levels of incident UVR are high. The extent of phototoxicity is strongly wavelength-dependent. While both UVA (320 nm–400 nm) and UVB (280 nm–320 nm) radiation can cause phototoxicity, the former is more relevant for activating PAH phototoxicity in aquatic organisms because it is received at higher irradiance levels and is less attenuated by seawater and dissolved substances (Barron, 2017).

The potential for photoactivation of a chemical is primarily determined by its ring conjugation and conformation. Anthracene is a three-ring PAH commonly present in fossil fuels and crude oil (Martins et al., 2011). Due to its strong hydrophobicity it easily accumulates in cell membranes, disrupting cellular metabolism (Aksmann et al., 2011; Huang et al., 1997). The toxic effects of anthracene to aquatic organisms can increase up to 1000-fold in the presence of UVR, while its structural isomer phenanthrene exhibits little photoenhanced toxicity (Peachey and Crosby, 1996; Pelletier et al., 1997; Willis and Oris, 2014). Photoenhanced toxicity can occur either as photomodification, whereby structural changes result in the formation of more toxic intermediates, or through the production of reactive oxygen species (ROS), known as photoexcitation (Barron, 2017).

Even in the absence of PAHs, UVA radiation can have severe impacts on a broad range of organisms. Effects of prolonged exposure include impaired metabolism, motility, growth and survival, as well as DNA damage (Hader et al., 2015). To minimize cell damage caused by ROS, organisms must be able to respond accordingly at a molecular level by activating DNA repair mechanisms and the antioxidant system, through changes in gene transcription and translation (Aksmann et al., 2014). Studies frequently analyze changes in the transcriptome to investigate physiological responses of organisms to a toxicant or stressor (Hutchins et al., 2010). Amongst the most important enzymes that reduce damage resulting from radicals are catalase (CAT) and superoxide dismutase (SOD) (Birben et al., 2012; Bolognesi and Cirillo, 2014).

An organism's physiological characteristics and developmental stage determine its susceptibility to UVR damage and photoenhanced toxicity. Early-life stages (for example, eggs, embryos and larvae) are often translucent, and although many posess photoprotective biochemicals, they remain particularly vulnerable to damaging radiation, as has been described for coral larvae (Aranda et al., 2011; Negri et al., 2016). Many scleractinian corals, such as the widespread and abundant genus *Acropora* spp., reproduce sexually during annual mass spawning events, where eggs and sperm are released into the water column, which after fertilization, develop into pelagic larvae that reach competency to settle and metamorphose into juvenile corals several days later (Jones et al., 2015). Settlement success of *Acropora* larvae can be crucial to the maintenance and recovery of coral reefs, but these submillimeter larvae are also particularly vulnerable to chemical stressors (Shaw et al., 2009). The present study used laboratory experiments to examine the effects of exposure to anthracene and phenanthrene on SOD enzyme activity, gene expression patterns, settlement success and survival of *Acropora tenuis* planula. A further aim was to establish if co-exposure to environmentally relevant intensities of UVA (320–400 nm) increases the harmful effects of anthracene and phenanthrene through phototoxicity.

2. Materials and methods

2.1. Coral collection and larval husbandry

Six gravid colonies of the scleractinian coral *Acropora tenuis* (Dana, 1846) were collected from reefs around Magnetic Island (19.157°S, 146.861°E) under Great Barrier Reef Marine Park Authority permit G12/35236.1 in October 2016. The corals were transported in seawater flow-through tanks at ambient temperature to the Australian Institute of Marine Science (Townsville, Australia), where, upon arrival, they were moved into outdoor aquaria supplied with flow-through seawater (27 °C) at the National Sea Simulator (SeaSim). On 19th October 2016, spawning occurred and the coral gametes were collected by gentle scooping from the water surface. Gamete collection and larvae culturing followed the methods described in Negri and Heyward (2000). Briefly, the corals were kept indoors under low light in aerated 380 l flow-through rearing tanks supplied with 1 μm filtered seawater at 27 °C. Larvae remained in those conditions until experiments commenced.

2.2. Chemical toxicant preparation and analysis

Treatment solutions of anthracene and phenanthrene were prepared by addition of analytical grade anthracene (Supelco Analytical, USA) and phenanthrene (Sigma-Aldrich, Germany) dissolved in dimethyl sulfoxide (DMSO) to 0.45 μm filtered seawater as well as pure DMSO to achieve a final solvent concentration of 0.01% v/v in each solution. Solutions were sonicated for 30 min prior to use to ensure PAH dissolution. Controls consisted of filtered seawater as well as a solvent control (FSW containing 0.01% v/v DMSO). The time-averaged PAH concentration for each experiment was determined from samples collected at the start and end of the 48 h exposure. Samples (100 ml) of treatment solutions were collected in 125 ml amber bottles with PTFE-lined caps from the highest concentration treatment. Solutions were preserved by adding dichloromethane (DCM) to a final concentration of ~20% (v/v) and stored at 4 °C. The samples were extracted three times with DCM and the extracts were dried with pre-combusted sodium sulfate (450 °C, 4 h), evaporated under nitrogen gas and filtered through pre-extracted cotton wool. Extracts were adjusted to 10 ml with DCM and analyzed using GC–MS in scan mode. A surrogate standard (*o*-terphenyl) (10 μg) was added to each sample at room temperature before extraction, and internal standards (biphenyl-d_{10}, phenanthrene-d_{10} and perylene-d_{12}) were added to the extracts prior to analysis. PAH concentrations and recovery (%) of surrogate standards are reported in Suppl. Table 1.

2.3. UVA radiation treatments

Two incubators (Thermoline Scientific, NSW, Australia) were equipped with a photosynthetically active radiation (PAR) source (Aqualina Blue 450 nm 10,000 K and 420 nm actinic LED strips, The Aquatic Life Product Company, Australia) generating an output of 57 μmol photons m^{-2} s^{-1} on a 12-h light: 12-h dark cycle. The treatment incubator was additionally equipped with UV fluorescent tubes (Deluxlite Blacklight Blue 18 W and Reptile One UVB 5.0 18 W). Incident UV radiation was measured with a PMA2100 data logging radiometer (Solar Light, USA) fitted with a UVA + UVB (280 nm–400 nm) and a UVB (280 nm–320 nm) sensor. The UVB sensor was used as a control to confirm that the larvae predominantly received UV radiation from the UVA spectrum as UVB is strongly attenuated by the borosilicate glass jars. Negligible UVC was emitted from the fluorescence tubes. Samples were positioned approximately 20 cm beneath the UV source. The incident UVA (320 nm–400 nm) and UVB (280 nm–320 nm) radiation inside the glass jars were 6.7 W m^{-2} and 0.1 W m^{-2}, respectively (see Suppl. Fig. 1 for spectral output). During the 48 h incubation period, samples were exposed to UV on a 10-h light:

14-h dark cycle, thereby receiving a daily UV dose of $240\,KJ\,m^{-2}\,d^{-1}$. Measurements performed in November 2016 at a mid-shelf and inner reef on the central Great Barrier Reef, QLD, showed that the intensity of UVA irradiance chosen for the experimental setup corresponds to conditions approximately 1 m below the surface at these sites (Nordborg et al., under review).

2.4. Mortality and metamorphosis experiments

To assess how PAH and UVA exposures affect the survival and metamorphosis success of *A. tenuis* larvae, we performed two subsequent incubation experiments: one with anthracene and one with phenanthrene. Seven solutions were prepared for each PAH in FSW: 600, 300, 150, 75, 37.5, 18.8, and $9.4\,\mu g\,l^{-1}$ for anthracene; and 900, 450, 225, 112.5, 56.3, 28.1 and $14.1\,\mu g\,l^{-1}$ for phenanthrene (all nominal concentrations; see Suppl. Table 1 for measured concentrations). Each solution contained 0.01% of the carrier solvent DMSO. PAH solutions (20 ml) were transferred into solvent-rinsed 25 ml borosilicate glass vials, while solvent and seawater controls were prepared as previously described (see 2.2). Fifteen *A. tenuis* larvae were added to each vial using plastic transfer pipettes and incubated under either $-UVA$ or $+UVA$ (see 2.3) for 48 h at 27 °C in the orbital shaker incubators at 70 rpm to prevent larval metamorphosis during exposure (Negri et al., 2016). To account for minor variations in radiation exposure inside the incubators, samples were randomly relocated twice daily. For each PAH concentration, solvent control and seawater control, six replicates (n = 6) were set up per radiation treatment. Following the exposures, the larvae including 10 ml of each solution were transferred into plastic 6-well cell culture plates. The planulae were observed under a dissecting microscope and the proportion of living (mobile) larvae was counted. To assess the ability of larvae to undergo metamorphosis into a juvenile coral, the peptide neurotransmitter GLW-amide was added to each well at a final concentration of 1.5 μM (Tebben et al., 2015). After 24 h at 27 °C, the number of metamorphosed larvae was counted.

2.5. SOD activity and gene expression experiments

2.5.1. Experimental setup and incubation

Enzymatic activity and gene expression responses of coral larvae to PAH exposure were tested for anthracene and phenanthrene in the absence ($-UVA$) and presence ($+UVA$) of UVA radiation. Solvent-cleaned 200 ml borosilicate glass jars were filled with 150 ml treatment solutions which contained nominal concentrations of $9.25\,\mu g\,l^{-1}$ and $37.5\,\mu g\,l^{-1}$ anthracene, or $37.5\,\mu g\,l^{-1}$ and $300\,\mu g\,l^{-1}$ phenanthrene, respectively (see Suppl. Table 1 for measured concentrations). Treatment concentrations were chosen as sub-lethal concentrations based on pilot exposures. FSW and solvent controls were included in each experiment. Approximately 200 *A. tenuis* larvae were transferred to each jar after which the containers were evenly distributed in the treatment ($+UVA$) and control ($-UVA$) incubators (see 2.3). Each orbital shaker incubator contained four $0\,\mu g\,l^{-1}$ controls, four replicates of each of the two treatment PAH concentrations, and two solvent controls each for protein assays and gene expression analysis. Samples were incubated for 48 h at 27 °C and 70 rpm. After incubation, protein assay samples were filtered onto a 200 μm mesh. The larvae were washed with 1 ml of filtered seawater and transferred into 1.5 ml microcentrifuge tubes along with 200 μl of ice-cold phosphate-buffered saline containing protease inhibitor cocktail (Sigma-Aldrich, Germany). Protein samples were processed on the same day. Larvae for gene expression analysis were filtered, transferred into 1.5 ml centrifuge tubes with 200 μl of RNAlater stabilization solution (Ambion, Austin, TX, USA) and kept at 4 °C for 24 h before being stored at -20 °C until further analysis.

2.5.2. Total protein and SOD activity assays

For the bioassays, samples were homogenized on ice with a micropestle and centrifuged at 4 °C and $13,000 \times g$ for 15 min. The resulting supernatants were used for the SOD assay, while for the protein assay 20 μl from each sample was firstly diluted in 80 μl of PBS. To normalize the enzyme activity data, total protein was quantified following the microplate protocol of the Coomassie Plus assay reagent (Thermo Scientific). Briefly, 10 μl of sample and protein standard were loaded in three technical replicates onto a 96 microwell plate and combined with 300 μl Coomassie Plus reagent. After 10 min of incubation at 22 °C, absorbance was determined at 595 nm using a Cytation 3 (BioTek, USA) microplate reader. A standard curve was generated to calculate total protein concentration as $\mu g\,protein\,ml^{-1}$.

An SOD determination kit (Sigma-Aldrich) was used to quantify superoxide dismutase activity. Samples and SOD standards from bovine erythrocytes (Sigma-Aldrich, cat. # S7571) were prepared according to the kit's protocol and incubated at 37 °C for 20 min before absorbance at 450 nm was measured using a Cytation 3 microplate reader. The% inhibition of each sample and SOD standard was calculated as described in the manual. Inhibition of the standards was plotted against the log-transformed SOD concentration in $U\,ml^{-1}$. SOD concentrations in the samples were interpolated from a sigmoidal four-parameter logistic (4PL) standard curve and activity was expressed as units (U) of enzyme activity per milligram of total protein ($U\,mg\,protein^{-1}$). The $0\,\mu g\,PAH\,l^{-1}$ data from the two experiments were pooled for both radiation treatments.

2.5.3. Gene expression: RNA extraction, cDNA synthesis and qPCR

Total RNA was extracted from each sample (which after the incubation contained approximately 100–200 larvae) using a NucleoSpin TriPrep extraction kit (Macherey-Nagel, Germany). RNA concentration was quantified using a NanoDrop 2000 spectrophotometer (Thermo Scientific) and its integrity and purity was confirmed using agarose gel electrophoresis. First-strand cDNAs were synthesized from 250 ng of total RNA using a SuperScript III First-Strand Synthesis SuperMix kit (Invitrogen) with $50\,ng\,\mu l^{-1}$ random hexamer primers. Eight genes of interest and one internal control gene (ICG) were selected (see Table 1). Three putative housekeeping genes (*Ctg1913*, *RiboL5*, *RiboL9*) were tested for the stability of their expression during UVA and PAH exposure. All primers were obtained from Sigma-Aldrich (Germany). *Ctg1913* exhibited the most stable expression and was consequently used as internal control gene. Expression levels were investigated in duplicates on 96-well plates with Power SYBR Green PCR Master Mix (Applied Biosystems). The samples were analyzed using a 7900HT Fast Real-Time PCR System (Applied Biosystems). Each qPCR reaction well contained 11.25 μl of Power SYBR Green PCR Master Mix, 0.33 mM forward primer, 0.33 mM reverse primer, 5.4 μl PCR-grade water and 2.5 μl of cDNA template, adding to a total of 20.5 μl. The qPCR conditions were 10 min denaturation at 95 °C, followed by 40 cycles of 20 s denaturation at 95 °C and 1 min annealing and extension at 60 °C. To check for nonspecific amplification, a melt curve analysis was performed after amplification with a temperature gradient from 65 °C to 95 °C. Specificity of the PCR amplification and amplicon product sizes were also validated using agarose gel electrophoresis. The target gene data were normalized against the expression levels of the internal control gene Ctg 1913 using the $2^{-\Delta\Delta CT}$ method (Livak and Schmittgen, 2001).

2.6. Statistical analysis

The mortality and metamorphosis data were analyzed and visualized in GraphPad Prism 7.0b (GraphPad Software Inc., CA, USA). Mean values along with SEM were calculated before the data were fitted using a non-linear inhibitor versus response curve with variable slope (four parameters) using least squares (ordinary) fit. Additionally, the PAH concentrations at which 50% reduction in mortality (relative LC_{50}) and metamorphosis (EC_{50}) occurred were interpolated for each of the two radiation treatments where possible.

Table 1
Accession number, amplicon size, primer efficiency, sequence and reference, and putative function of eight target genes and one internal control gene (ICG) included in the RT-qPCR assay. Internal control gene is indicated by asterisk (*). The p53 primer was designed by the authors using the primer design tool Primer-BLAST (NCBI).

Protein name	Gene abbreviation	Accession No.	Amplicon size (bp)	Primer efficiency (%)	Primer sequence	Primer reference	Putative function
Green fluorescent protein	Gfp	AY646066	56	90.5	(F)TTGGCCAAAGTGCAAAAGG (R)ATGAGCCGCAGCATGTTCT	Yuyama et al. (2012a)	Photoprotection, Reactive oxidant quenching
Red fluorescent protein	Rfp	AB626607	54	99.2	(F)ACCGGATGGAAGGGTGTGT (R)GCCGTGGCCCGTGAT	Yuyama et al. (2012a)	Photoprotection, Reactive oxidant quenching
Oxidative stress-responsive protein	Ox stress	DC999943	59	93.0	(F)TGACCACCACCCCTGAGGAA (R)GCTTGGGAATGTAAAGCAACTGA	Yuyama et al. (2012a)	Involved in antioxidant defense system
Heat shock protein 90	Hsp90	DC999947	64	87.5	(F)GATGCGACTGGCATGAACT (R)GAGACCTCTCTTGTCCTCTGGTT	Yuyama et al. (2012b)	Protein folding and stabilization
Heat shock protein 70	Hsp70	DY585921	99	97.6	(F)TGCTGCGTTCACCTTCAAACA (R)GCAACACAACAATTCCCACGA	Csaszar et al. (2009)	Protein folding and stabilization
Superoxide dismutase	MnSod	DY581262	101	93.5	(F)CGATGCCTTGAAACCTGCAA (R)TTTCTTCGGCCGCGTTAAG	Csaszar et al. (2009)	Involved in antioxidant defense system
Catalase	Cat	EZ013640	177	92.5	(F)AGGTGCACACTATAGAATAATCCGCTGATTACTGTTGGC (R)GTACGACTCACTATAGGGAGGCGACCCTGCAACATCTTAT	Bay et al. (2013)	Involved in antioxidant defense system
Tumor protein p53	p53	XM_015896829	114	97.9	(F)TGGTCTTTGGAAACTCAGCCC (R)TTGTTAGAAACCGCACGGGA	designed by authors	Regulates cell growth, DNA repair and apoptosis
Unknown transcript*	Ctg1913	DY585358	104	93.2	(F) GTGCGTGCTGCTCCCATATTAC (R) TGAAGTCGTGGTCGTAGTTG	Csaszar et al. (2009)	unknown transcript

Using JMP 13.1 (SAS Institute Inc. Cary, North Carolina, USA), a full-factorial generalized linear model (GLM) with normal distribution and an identity link function was fitted to compare the main effects of anthracene/phenanthrene concentration and UVA treatment and their interactive effect on SOD activity and gene expression (one model per gene). This analysis was followed by multi-comparison of each data pair using Student's *t*-test to identify differences between individual experimental treatments. To test the data for normal distribution and homogeneity of variances, a Shapiro-Wilks test and Levene test were used, respectively. Where necessary, the data were log-transformed to obtain a normal distribution. Differences were considered to be significant at $p < 0.05$. Additionally, a principal component analysis (PCA) was performed on the gene expression data set to identify distinctly separate treatments.

3. Results

3.1. Larvae mortality and metamorphosis

For the anthracene experiment, larval survival after 48 h was on average $96 \pm 2\%$ in the −UVA control samples (Fig. 1A). Survival decreased gradually with increasing anthracene concentration to a low of $39 \pm 3\%$ at $378 \, \mu g \, l^{-1}$ (−UVA). The presence of anthracene and UVA had a substantial effect on larval survival. At each anthracene concentration, mean survival was reduced by over 20% in the +UVA samples compared to the −UVA samples. None of the larvae survived when exposed to UVA and anthracene $\geq 189 \, \mu g \, l^{-1}$ (Fig. 1A). The LC_{50} for anthracene was reduced from $44 \, \mu g \, l^{-1}$ (95% CI: 28–69) to $18.1 \, \mu g \, l^{-1}$ (95% CI: 15–22) in the presence of UVA.

Phenanthrene had far less impact on coral planulae survival in comparison to anthracene (Fig. 1B). Larval survival of controls was 95% and 97% in the absence and presence of UVA. At the highest phenanthrene concentration ($872 \, \mu g \, l^{-1}$) larval survival was $89 \pm 4\%$ and $82 \pm 6\%$ for the −UVA and +UVA treatments, respectively. Additionally, UVA radiation had no significant effect on the survival rate of controls.

In the anthracene experiment, metamorphosis success was $55 \pm 6\%$ and $56 \pm 6\%$ for solvent control larvae in the absence and presence of UVA, respectively. Metamorphosis decreased with increasing anthracene concentrations, and this inhibition was more pronounced in the presence of UVA (Fig. 1C). The EC_{50} for anthracene decreased from $45 \, \mu g \, l^{-1}$ (95% CI: 18–126) to $6.3 \, \mu g \, l^{-1}$ (95% CI: 5.8–6.8) in the presence of UVA. In the phenanthrene experiment, the mean metamorphosis rate for the controls was lower than in the anthracene experiment: $31 \pm 3\%$ −UVA and $45 \pm 4\%$ +UVA (Fig. 1D). Metamorphosis success appeared to increase slightly (to $42 \pm 7\%$ −UVA and $53 \pm 9\%$ +UVA) at the lowest phenanthrene concentration ($13.6 \, \mu g \, l^{-1}$) before decreasing as phenanthrene concentration increased (Fig. 1D). Co-exposure to UVA had little influence on the inhibition of phenanthrene to metamorphosis (EC_{50} of $91 \, \mu g \, l^{-1}$ (95% CI: 42–204) and $66 \, \mu g \, l^{-1}$ (95% CI: 40–112) in the absence and presence of UVA, respectively).

3.2. SOD activity

Anthracene exposure had a significant effect on SOD activity in coral larvae, as identified by the GLM ($\chi^2_{(2, \, N = 32)} = 10.951$, $p < 0.01$). The highest SOD activity ($9.3 \pm 6.3 \, U \, mg^{-1}$) was found in the $0 \, \mu g \, l^{-1}$ −UVA control larvae, significantly more ($t(26) = -2.42$, $p < 0.05$) than the $17 \, \mu g \, l^{-1}$ anthracene samples from the −UVA ($3.3 \pm 1.5 \, U \, mg^{-1}$) ($t(26) = -2.76$, $p = 0.010$) and +UVA treatments ($4.0 \pm 0.2 \, U \, mg^{-1}$) ($t(26) = -2.42$, $p < 0.05$). UVA did not have a significant effect on enzyme activity compared to the corresponding −UVA treatment for any anthracene concentration used.

For the phenanthrene experiment, the highest SOD activity was identified in the $0 \, \mu g \, l^{-1}$ −UVA treatment ($9.3 \pm 6.3 \, U \, mg^{-1}$), while
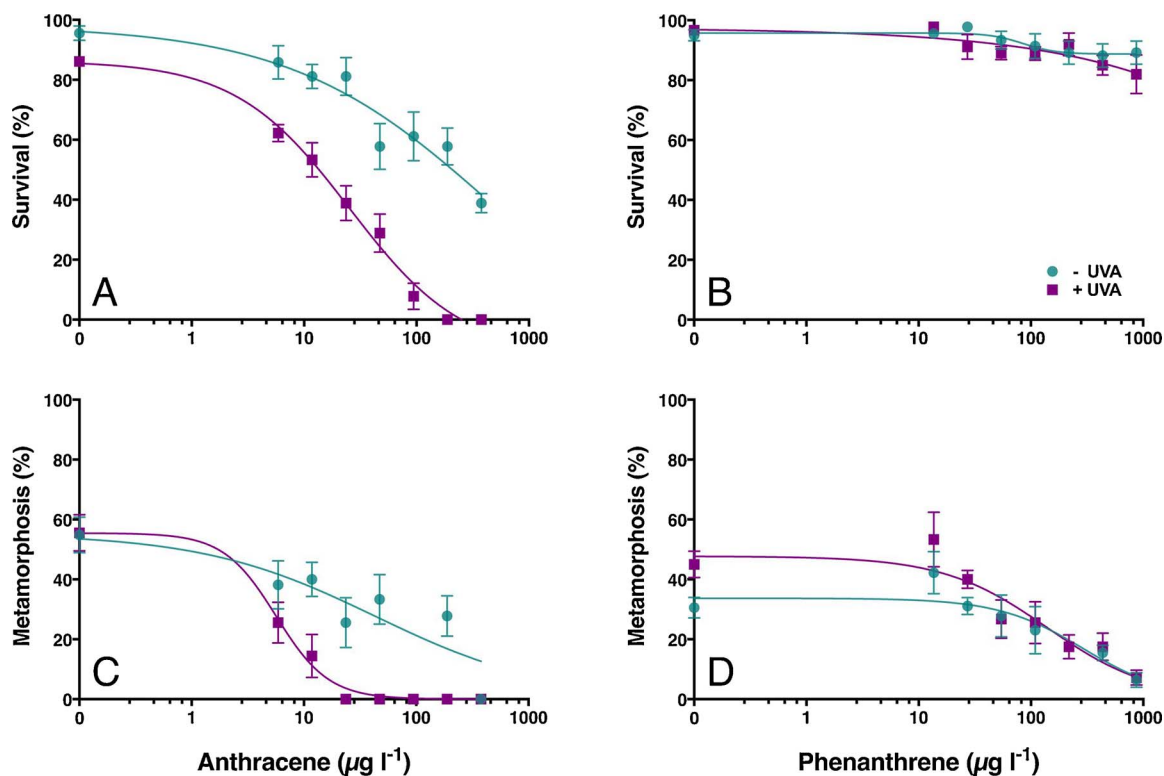
Fig. 1. Survival (%) after 48 h and metamorphosis (%) after 72 h in *A. tenuis* larvae exposed to anthracene (A, C) and phenanthrene (B, D) under −UVA (green circles) or +UVA (purple squares) radiation. Plotted PAH concentrations are calculated, time-averaged values. Error bars indicate SEM (treatments n = 6, controls n = 12). (For interpretation of the references to color in this figure legend, the reader is referred to the web version of this article.)

the 39 $\mu g \, l^{-1}$ +UVA treatment showed the lowest activity (6.6 ± 1.3 U mg^{-1}) (Fig. 2). Mean SOD activity decreased with increasing phenanthrene concentration in the −UVA treatments. No apparent pattern was observed for the larvae exposed to UVA. No significant differences in SOD activity were observed between treatment groups and no interactions or main effects due to phenanthrene concentration and UVA radiation were detected by the GLM analysis.

3.3. Gene expression

The presence of anthracene had a highly significant effect (p < 0.01) on the expression of most target genes, except *MnSod* and *p53*. The strongest response was observed for *Hsp70*, *Hsp90* and *Cat*, where anthracene exposure enhanced gene transcription by more than

three-fold compared to controls (Fig. 3). The expression of *Hsp90* in particular amplified with increasing anthracene concentration. The GLM identified that UVA only affected the expression of *Gfp* significantly ($\chi^2_{(1, \, N = 32)}$ = 9.011, p < 0.001), while no effect was observed for any of the other target genes. Phenanthrene exposure only affected the expression of *Rfp* significantly, reducing transcription by less than one-fold (apart from samples exposed to the 39 $\mu g \, l^{-1}$ −UVA treatment which were unaffected) (Fig. 3).

Interactive effects between UVA and anthracene varied with anthracene concentration. Catalase and the oxidative stress gene were significantly upregulated at the lower dosage of 4 $\mu g \, l^{-1}$ (Fig. 3), and *Hsp70* was downregulated at the higher dosage of 17 $\mu g \, l^{-1}$. However, in the absence of PAHs, exposure to UVA radiation only caused *p53* to be differentially expressed.
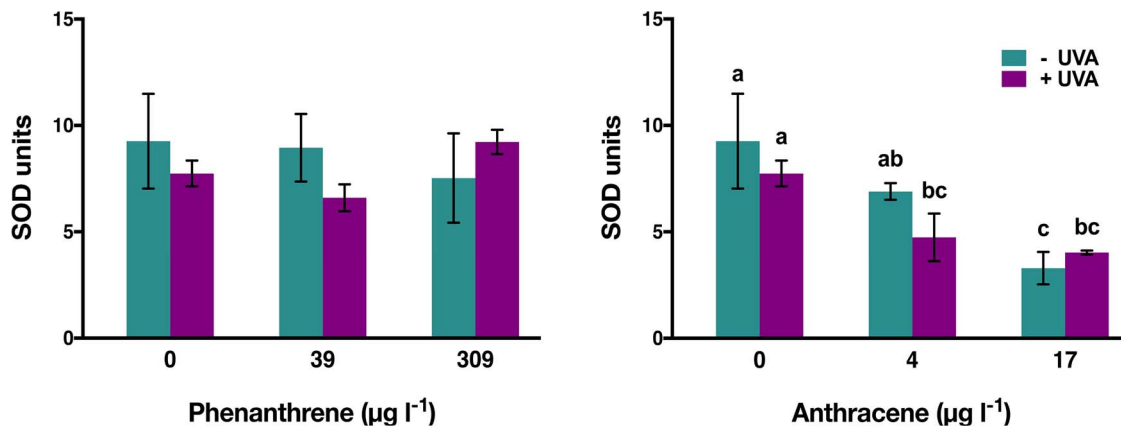

Fig. 2. Superoxide dismutase activity (SOD units per mg of total protein) in response to phenanthrene and anthracene under −UVA (green bars) or +UVA (purple bars) conditions. PAH concentrations are time-averaged values. Error bars represent SEM (n = 4; except 0 $\mu g \, l^{-1}$ where n = 8). Letters above bars indicate results of multiple comparison Student's *t*-tests. Bars that do not share a common letter were significantly different from each other (p < 0.05). For phenanthrene, no difference was found between any of the treatments. (For interpretation of the references to color in this figure legend, the reader is referred to the web version of this article.)
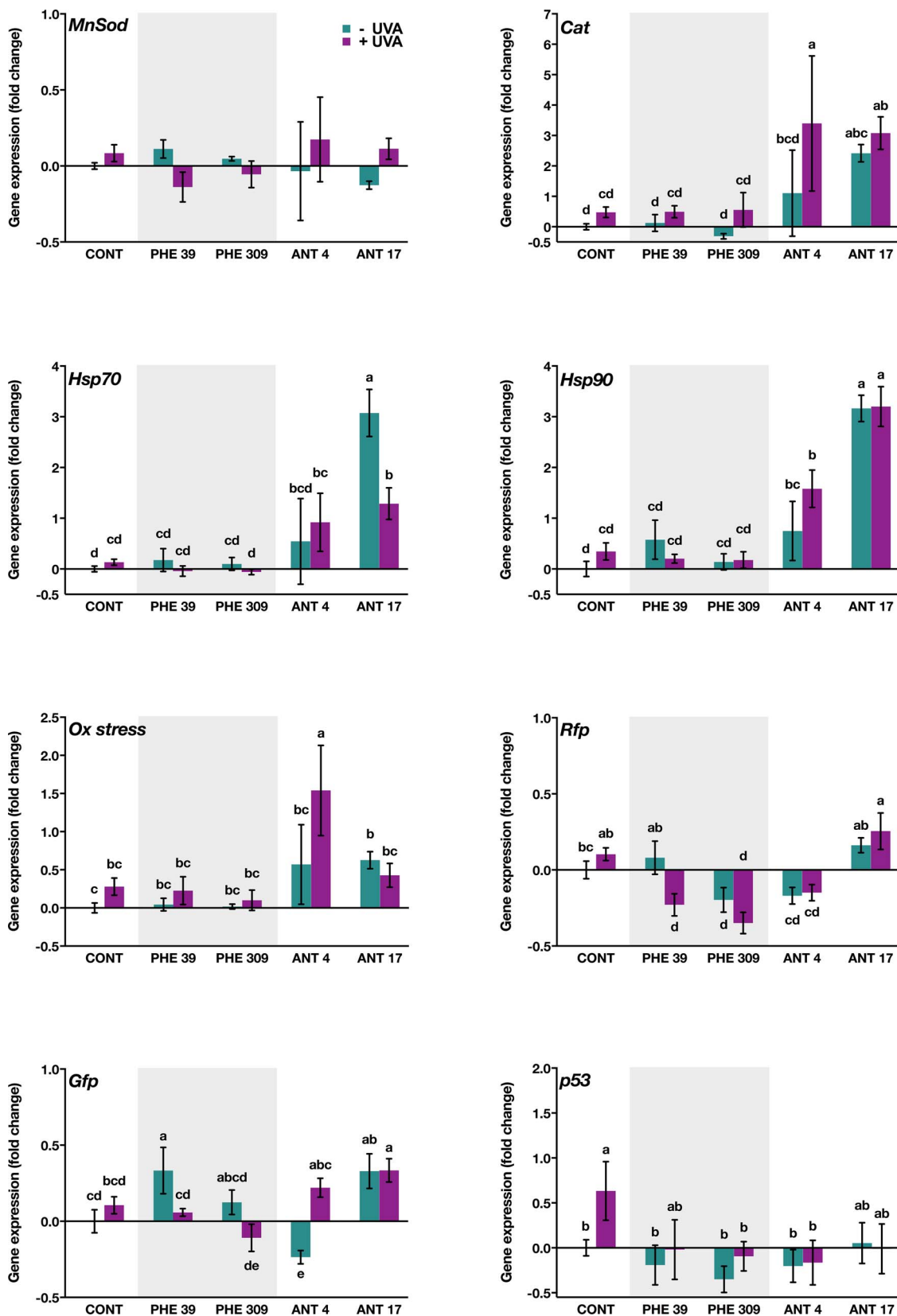
Fig. 3. Expression of eight target genes (see Table 1) in *A. tenuis* larvae exposed to anthracene (ANT) or phenanthrene (PHE) under −UVA (green bars) and +UVA (purple bars) as determined by quantitative PCR analysis. Numbers following PHE and ANT denote time-averaged PAH concentrations in µg l^{-1}. Data were normalized against expression levels of the internal control gene *Ctg1913* (data not displayed). Change in expression is displayed as fold change compared to the PAR control sample. Note the difference in y-axis scales. Treatment samples were analyzed in triplicates (n = 3). Controls and solvent controls were merged since there were not significantly different for any of the genes (Student's *t*-test, p > 0.05), thereby totaling six replicates (n = 6). Letters above bars indicate the results from multiple comparison Student's *t*-tests. Bars that do not share a common letter are significantly different from each other (p < 0.05). Error bars indicate SEM. Note that for *MnSod* none of the treatments were significantly different from each other. (For interpretation of the references to color in this figure legend, the reader is referred to the web version of this article.)
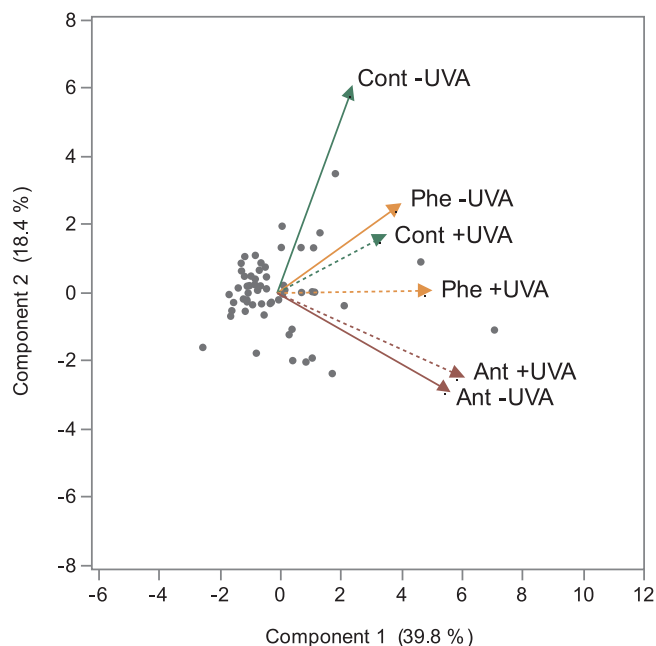
Fig. 4. Principal component analysis (PCA) of the gene expression data set. Displayed are the vectors for the six exposure treatments: controls without PAHs (Cont, in green), phenanthrene (Phe, in orange) and anthracene (Ant, in red) exposed to PAR and UVA (+ UVR, dotted line) and PAR-only (− UVR, solid line). (For interpretation of the references to color in this figure legend, the reader is referred to the web version of this article.)

In summary, the presence of PAHs affected gene expression in *A. tenuis* larvae more than the exposure to UVA. In particular, anthracene changed gene transcription, while phenanthrene had little or no effect on expression patterns. The principal component analysis strongly supported this finding, as the directions of the anthracene vectors are distinct from those of the other treatments (Fig. 4). Superoxide dismutase (*MnSod*) was the only gene in which expression was unaffected by the presence of a PAH or exposure to UVA.

4. Discussion

Coral larvae were more sensitive to anthracene than phenanthrene, with lower concentrations of anthracene causing mortality and reducing larval metamorphosis than phenanthrene. The same effect was observed in the expression patterns of some stress-related genes (particularly *Hsp70*, *Hsp90* and *Cat*). However, there was little effect of either PAH on SOD enzyme activity. UVA exposure induced a strong phototoxic impact for anthracene, reducing the LC_{50} by more than two-fold and the EC_{50} for metamorphosis more than seven-fold. In contrast, UVA only elicited a small phototoxic effect on phenanthrene. Overall this study revealed strong phototoxicity at low anthracene concentrations to coral larvae, demonstrated in both larval development and gene expression patterns. These results also highlight the sensitivity of expression data from genes recognized as stress response biomarkers, which shed light on the pressure-response pathways for phototoxicity, and could be applied as diagnostics and sub-lethal indicators for coral stress following oil spills.

4.1. Larval mortality and metamorphosis

Anthracene was far more toxic to coral larvae than phenanthrene, and co-exposure to UVA enhanced the damaging effects of anthracene but not phenanthrene. Lethal effects of petroleum products on corals have previously been reported for larvae and adult fragments of several scleractinian species (as reviewed and summarised by Turner and Renegar (2017)). The acute toxic mechanism of PAHs is widely

assumed to be narcosis, and the target lipid model predicts that anthracene should be more toxic than phenanthrene (McGrath and Di Toro, 2009; Redman et al., 2012). However, other modes of action are possible such as increased ROS production (reviewed in Billiard et al. (2008)), and while survival represents a critical stress response, it is (by definition) the least sensitive indicator of stress. The LC_{50}s for anthracene and phenanthrene in the absence of UVA was higher than the EC_{50}s for larval metamorphosis, confirming the higher sensitivity of larval metamorphosis as an ecologically relevant endpoint for PAH toxicity (Negri et al., 2016). Coral larvae metamorphose and settle after sensing the presence of chemical components found in crustose coralline algae, amongst other relevant metamorphosis-inducing cues (Heyward and Negri, 1999). Reduced metamorphosis success could result from an impairment of the mechanisms by which coral larvae can detect the presence of metamorphosis cues (Negri and Heyward, 2000). However, in the present study larval metamorphosis was initiated using the peptide GLW-amide, which bypasses the natural chemoreception process (Grasso et al., 2011) and therefore inhibition represents a strong physiological impairment of the larvae's ability to metamorphose. Kushmaro et al. (1997) observed that planulae of the octocoral *Heteroxenia fuscescens* could not undergo metamorphosis when exposed to crude oil due to metamorphosis inhibition as a result of severe larval deformities. We likewise observed deformities (not quantified) in some larvae of the PAH treatments, suggesting that a disruption to mitosis in developing larvae may have contributed to metamorphosis failure.

UVA exposure increased the toxicity of anthracene by over two-fold for survival and seven-fold for metamorphosis. Choi and Oris (2000) suggested that the photoinduced toxicity of anthracene results from an increase in ROS production, which ultimately leads to lipid peroxidation and potentially mortality. The impact of anthracene phototoxicity on survival was first described for freshwater fish (Bowling et al., 1983), while subsequent studies found that photoenhanced damage by PAHs to aquatic organisms is a widespread phenomenon. For cnidarians, Tarrant et al. (2014) identified that when juveniles of the sea anemone *Nematostella vectensis* were shielded from UVR, the acute toxicites of benzo[a]pyrene, pyrene and fluoranthene were significantly reduced. Larvae of the coral *Fungia scutaria* also showed high sensitivity to phototoxicity (Peachey and Crosby, 1996), while polyps of the anemone *Anthopleura aureoradioata* exhibited a high tolerance (Ahrens and Hickey, 2002). Phototoxicity to *Acropora tenuis* larvae by water accommodated fractions of light crude oil, heavy fuel oil and diesel also increased by two- to three-fold in the presence of UVR (Negri et al., 2016; Nordborg et al., under review). Early life stage organisms, and particularly transparent larvae like aposymbiotic coral larvae, are prone to the phototoxic effects of PAHs and oil (Bellas et al., 2008; Lyons et al., 2002), highlighting the potential impact of this phenomenon on larval health and subsequent coral recruitment. Other reproductive stages of coral have also shown to be affected by co-exposure to PAHs and UVR, including a significant reduction in female gonad production by *Stylophora pistillata* colonies subjected to crude oil (Rinkevich and Loya, 1979).

In contrast to the strong influence of UVA on anthracene, the co-exposure of larvae to phenanthrene and UVA did not result in phototoxic effects on survival or metamorphosis. The lack of phototoxicity is likely due to differences in the ring conjugation and intermolecular forces of these PAHs, which affect their UV absorption properties (Wang et al., 2009), and these results are broadly consistent with a low influence of UVA on gene responses. The fact that not all PAHs are phototoxic may help explain why exposure to UVR increased the toxicity of PAH mixtures (water accommodated fractions of oils and fuels) by two to three-fold (Negri et al., 2016), while some individual PAHs can increase in toxicity by up to seven-fold (this study).

4.2. SOD activity

SOD is an important enzymatic ROS scavenger, which facilitates the

dismutation of superoxide to oxygen and hydrogen peroxide, which in turn becomes substrate for the enzyme catalase. Hence, enhanced oxidative stress causes organisms to increase the production of SOD to mitigate cell damage (Alscher et al., 2002; Michiels et al., 1994; Mittler, 2002). For corals, thermal stress, changes in salinity, high doses of ultraviolet radiation or a combination of these factors can all lead to increased activity of enzymatic antioxidants (Downs et al., 2002; Levy et al., 2006; Shick et al., 1995). However, in the present study the exposure to UVA radiation did not affect SOD activity of coral larvae. This finding would suggest that the moderate intensity of UVA ($6.7\,\mathrm{W\,m^{-2}}$) did not affect superoxide anion generation compared to control samples. Alternatively, the presence of UVA may have triggered the larvae to express more SOD, but the UVA caused photoinactivation of the enzyme (Linan-Cabello et al., 2010; Obermüller et al., 2005), such that SOD activity remained at an equilibrium level close to that of the control samples. However, if this opposing interplay had been the case, SOD gene expression levels would have been higher in the larvae exposed to UVA than in the larvae exposed to PAR only. Since there was no difference between *MnSod* expression levels (see 4.3), we conclude that, although ecologically relevant (Nordborg et al., under review), the experimental UVA intensity did not cause a significant increase in superoxide anion production.

Of the two PAHs tested, only anthracene exposure caused a change (reduction) in the activity of SOD. This reduced SOD activity contrasts the findings of Aksmann and Tukaj (2004), who reported enhanced total SOD activity in cells of the green alga *Scenedesmus armatus* exposed to anthracene. While SOD gene transcription and enzyme activity are commonly increased under stress conditions to minimise cell damage, some studies identified that superoxide dismutation was suppressed after anthracene exposure. Zbigniew and Wojciech (2006) reported that at a concentration of $250\,\mathrm{\mu g\,l^{-1}}$, anthracene reduced the enzymatic reaction of the two superoxide dismutase isoforms Fe- and Mn-SOD in cells of the alga *Scenedesmus microspina*. One possible explanation for this response may be that anthracene damaged the enzyme. Anthracene can exert its toxicity on living organisms through the induction of conformational changes in biological membranes or proteolysis, which ultimately leads to ROS overproduction and metabolism disruption (Almeda et al., 2013; Duxbury et al., 1997; Grundy et al., 1996). Reactive oxygen species have the potential to damage antioxidant proteins if stress levels are beyond mitigation capacity, as has been observed for the relatively labile enzyme, ascorbate peroxidase (APX) (de Pinto et al., 2006). While SOD is known to be less prone to damage than APX, even the relatively stabile SOD can be damaged by ROS activity, as shown for the isoform Mn-SOD (Cyrne et al., 2003). Additionally, the concentrations of anthracene used in our experiment were higher compared to those in other studies, so it is possible that anthracene directly damaged SOD. Alternatively, enzyme activity may have been reduced through means of post-translational regulation triggered by the presence of anthracene. In contrast, SOD activity was not affected by the high concentration of phenanthrene. The less pronounced effect of phenanthrene on the physiology of *A. tenuis* larvae was expected since its toxicity has been reported as relatively low compared to anthracene (Krylov et al., 1997; Lee et al., 2003), and this was confirmed in the present study where phenanthrene LD_{50} and EC_{50}s were higher for coral larval mortality and metamorphosis, respectively.

4.3. Gene expression

The focus of gene expression analysis in this study was on applying recognized biomarkers of stress in scleractinian corals, including heat shock proteins, fluorescent proteins, superoxide dismutase and other antioxidant proteins (Bhaskaran et al., 1999; Downs et al., 2000; Smith-Keune and Dove, 2008). The first line of defense against oxidative stress is the enzyme SOD, which dismutases superoxide anions to the less harmful molecule hydrogen peroxide, a substrate and signaling molecule for the induction of heat shock proteins (HSPs) and catalase (Foyer

and Noctor, 2005). The enzymatic reactions of SOD, HSPs and catalase are therefore highly dependent on each other. No change in *MnSod* gene expression was observed in any of the treatments in comparison to the control samples, which suggests unchanged oxidative stress levels; however, enhanced expression of *Hsp70*, *Hsp90* and *Cat* was evident when anthracene was present. Catalase is responsible for the conversion of reactive and harmful hydrogen peroxide into oxygen and water (Levy et al., 2006), and is considered one of the most important radical scavenger enzymes in cnidarians along with SOD (Higuchi et al., 2008; Nii and Muscatine, 1997; Shick et al., 1995). Our findings therefore strongly suggest that the coral larvae overexpressed heat shock proteins and catalase (and increased SOD activity) in response to elevated levels of ROS due to the anthracene exposure.

For cnidarians, it has been reported that high temperature (Csaszar et al., 2009; Souter et al., 2011; Voolstra et al., 2009) and combined PAH-UV exposure (Tarrant et al., 2014) can cause increased transcription of genes such as *Sod, Hsp70* and *Cat*, indicative of an oxidative stress response, while the antioxidant activity of the corresponding enzymes can be altered by environmental stressors including pH variations (Soriano-Santiago et al., 2013), increased UVA radiation (Levy et al., 2006) and exposure to PAHs (Ramos and Garcia, 2007). Photo-enhanced upregulation in the transcription of genes encoding antioxidant enzymes was not observed for anthracene in this study, except for *Cat* and *Ox stress* at $4\,\mathrm{\mu g\,l^{-1}}$ anthracene (but not at higher anthracene concentration). In contrast, phenanthrene did not induce any oxidative stress response based on the expression patterns of *MnSod*, *Cat*, *Hsp70* and *Hsp90*.

Fluorescent proteins (FPs) can alleviate the photoinhibitory effects of UVA and hyperthermal stress, which otherwise may lead to bleaching in symbiotic corals (Salih et al., 2000). Here, a small (< 0.5 fold) but significant reduction in the expression of *Rfp* in UVA-treated coral larvae exposed to the lower phenanthrene concentration was observed, while at the higher phenanthrene concentration *Rfp* expression was significantly reduced for both UVA treatments. Smith-Keune and Dove (2008) have suggested that the expression pattern of fluorescent protein genes can be used as an early indicator of abiotic stress in corals. The authors identified that the gene of a *Gfp* homolog was underexpressed in adult *A. millepora* polyps in response to hyperthermal conditions, even before heat stress-induced metabolic or cellular damage was detectable. Gene downregulation in response to heat stress has also been described for the fluorescent protein homolog DsRed-type FP in aposymbiotic *A. millepora* larvae (Rodriguez-Lanetty et al., 2009). Besides having a photoprotective role in cnidarians, FPs might additionally be capable of quenching reactive oxygen species. Bou-Abdallah et al. (2006) described that GFP from the hydrozoan *Aequorea victoria* has SOD-like properties due to its ability to scavenge superoxide anions, while fluorescent proteins in Caribbean corals have shown signs of hydrogen peroxide quenching (Palmer et al., 2009). In our experiment, the expression patterns of *Rfp* and *Gfp* showed little evidence of PAH-induced stress, apart from the significant downregulation of *Gfp* in the phenanthrene treatment.

When intracellular oxidative stress in anthozoans cannot be managed by protective mechanisms including those discussed above, DNA damage can be irreparable. Subsequently, cells are removed through the initiation of necrosis (premature cell death), or organisms can actively induce apoptosis (programmed cell death) (Dunn et al., 2004; Richier et al., 2006). An essential protein in cell-growth mediation in many organisms is the tumor suppressor p53 (Hartwell and Kastan, 1994). Beside its role in apoptosis, p53 additionally contributes to regulatory pathways of DNA repair and mutation prevention, thereby protecting genome integrity (Helton and Chen, 2007; Rhee et al., 2013). Several studies have reported upregulation of p53 by aquatic organisms in response to abiotic stressors including elevated temperature (Lesser and Farrell, 2004), genotoxic chemicals (Banni et al., 2009; Hwang et al., 2010) as well as ultraviolet (Sandrini et al., 2009) and ionizing (Rhee et al., 2013) radiation. While we found *p53* overexpressed in

coral larvae from the +UVA treatment, indicating strong cellular stress responses, the presence of PAHs mostly caused downregulation of *p53*. Banni et al. (2009) suggested that contradicting p53 gene expression patterns might be due to the differences in the nature of the stressors (i.e. UVR and PAHs), the health state of cells (healthy versus cancerous cells), or be dependent on concentration and exposure duration. Additionally, specific PAHs such as benzo[a]pyrene can cause DNA strand breaks resulting in cell mortality or somatic mutations (Shackelford et al., 1999). In the +UVA controls, *p53* was possibly overexpressed to repair UV-induced DNA damage, modulate cell growth or initiate apoptosis where necessary. In some of the treatments, the exposure to PAHs may have disrupted this response through the mutation or drastic downregulation of the p53 gene, which ultimately may have led to an increase in the number of damaged cells, larval mortality and metamorphosis failure. However, in order to establish the exact mechanisms, it is necessary to monitor p53 protein levels in addition to measuring p53 mRNA levels, since the activity of p53 is known to be regulated both translationally and through post-translational modifications (reviewed in Kruse and Gu (2009)).

4.4. Conclusions

In summary, we found that anthracene was significantly more toxic to *A. tenuis* larvae than phenanthrene, and only anthracene exhibited increased phototoxicity under UVA exposure. It is apparent that while gene expression patterns and enzyme activity data can inform us on the likely mechanisms of stress, they do not necessarily provide reliable information on the severity of adverse impacts on an organism's fate following contaminant exposure. For example, even though there were few indications of phototoxic influence on the enzyme activity and only minor signs in the gene expression results, the metamorphosis assay clearly highlighted the strong effect of UVA radiation on anthracene toxicity and ultimately larval development. This finding emphasizes the necessity to develop a broader suite of sub-lethal toxicity indicators to better understand the mechanisms and impacts of organic contaminants and ultraviolet radiation on the survival and metamorphosis success of coral larvae.

Acknowledgements

Appendix A. Supplementary data

Supplementary data associated with this article can be found, in the online version, at https://doi.org/10.1016/j.aquatox.2018.03.008.

References

Ahrens, M.J., Hickey, C.W., 2002. UV-photoactivation of polycyclic aromatic hydrocarbons and the sensitivity of sediment-dwelling estuarine organisms, UV radiation and its effects: an update 2002. Proceedings of a Workshop Held in Christchurch. RSNZ Miscellaneous Series 63–65.
Aksmann, A., Tukaj, Z., 2004. The effect of anthracene and phenanthrene on the growth, photosynthesis, and SOD activity of the green alga *Scenedesmus armatus* depends on the PAR irradiance and CO2 level. Arch. Environ. Contam. Toxicol. 47, 177–184.
Aksmann, A., Pokora, W., Baścik-Remisiewicz, A., Dettlaff-Pokora, A., Wielgomas, B., Dziadziuszko, M., Tukaj, Z., 2014. Time-dependent changes in antioxidative enzyme expression and photosynthetic activity of *Chlamydomonas reinhardtii* cells under acute exposure to cadmium and anthracene. Ecotoxicol. Environ. Saf. 110, 31–40.
Almeda, R., Wambaugh, Z., Chai, C., Wang, Z., Liu, Z., Buskey, E.J., 2013. Effects of crude oil exposure on bioaccumulation of polycyclic aromatic hydrocarbons and survival of adult and larval stages of gelatinous zooplankton. PLoS One 8, e74476.
Alscher, R.G., Erturk, N., Heath, L.S., 2002. Role of superoxide dismutases (SODs) in controlling oxidative stress in plants. J. Exp. Bot. 53, 1331–1341.
Aranda, M., Banaszak, A.T., Bayer, T., Luyten, J.R., Medina, M., Voolstra, C.R., 2011. Differential sensitivity of coral larvae to natural levels of ultraviolet radiation during the onset of larval competence. Mol. Ecol. 20, 2955–2972.
Banni, M., Negri, A., Rebelo, M., Rapallo, F., Boussetta, H., Viarengo, A., Dondero, F., 2009. Expression analysis of the molluscan p53 protein family mRNA in mussels (*Mytilus* spp.) exposed to organic contaminants. Comp. Biochem. Physiol. C 149, 414–418.
Barron, M.G., 2017. Photoenhanced toxicity of petroleum to aquatic invertebrates and fish. Arch. Environ. Contam. Toxicol. 40–46.
Bay, L.K., Guerecheau, A., Andreakis, N., Ulstrup, K.E., Matz, M.V., 2013. Gene expression signatures of energetic acclimatisation in the reef building coral *Acropora millepora*. PLoS One 8, e61736.
Bellas, J., Saco-Alvarez, L., Nieto, O., Beiras, R., 2008. Ecotoxicological evaluation of polycyclic aromatic hydrocarbons using marine invertebrate embryo-larval bioassays. Mar. Pollut. Bull. 57, 493–502.
Bhaskaran, A., May, D., Rand-Weaver, M., Tyler, C.R., 1999. Fish p53 as a possible biomarker for genotoxins in the aquatic environment. Environ. Mol. Mutagen. 33, 177–184.
Billiard, S.M., Meyer, J.N., Wassenberg, D.M., Hodson, P.V., Di Giulio, R.T., 2008. Nonadditive effects of PAHs on early vertebrate development: mechanisms and implications for risk assessment. Toxicol. Sci. 105, 5–23.
Birben, E., Sahiner, U.M., Sackesen, C., Erzurum, S., Kalayci, O., 2012. Oxidative stress and antioxidant defense. World Allergy Organ. J. 5, 9–19.
Bolognesi, C., Cirillo, S., 2014. Genotoxicity biomarkers in aquatic bioindicators. Curr. Zool. 60, 273–284.
Bou-Abdallah, F., Chasteen, N.D., Lesser, M.P., 2006. Quenching of superoxide radicals by green fluorescent protein. Biochim. Biophys. Acta 1760, 1690–1695.
Bowling, J., Leversee, G., Landrum, P., Giesy, J., 1983. Acute mortality of anthracene-contaminated fish exposed to sunlight. Aquat. Toxicol. 3, 79–90.
Choi, J., Oris, J.T., 2000. Evidence of oxidative stress in bluegill sunfish (*Lepomis macrochirus*) liver microsomes simultaneously exposed to solar ultraviolet radiation and anthracene. Environ. Toxicol. Chem. 19, 1795–1799.
Csaszar, N.B.M., Seneca, F.O., van Oppen, M.J.H., 2009. Variation in antioxidant gene expression in the scleractinian coral *Acropora millepora* under laboratory thermal stress. Mar. Ecol. Prog. Ser. 392, 93–102.
Cyrne, L., Martins, L., Fernandes, L., Marinho, H.S., 2003. Regulation of antioxidant enzymes gene expression in the yeast *Saccharomyces cerevisiae* during stationary phase. Free Radic. Biol. Med. 34, 385–393.
de Pinto, M.C., Paradiso, A., Leonetti, P., De Gara, L., 2006. Hydrogen peroxide, nitric oxide and cytosolic ascorbate peroxidase at the crossroad between defence and cell death. Plant J. 48, 784–795.
De'ath, G., Fabricius, K.E., Sweatman, H., Puotinen, M., 2012. The 27-year decline of coral cover on the Great Barrier Reef and its causes. Proc. Natl. Acad. Sci. U. S. A. 109, 17995–17999.
Dodge, R.E., Wyers, S.C., Frith, H.R., Knap, A.H., Smith, S.R., Sleeter, T.D., 1984. The effects of oil and oil dispersants on the skeletal growth of the hermatypic coral *Diploria strigosa*. Coral Reefs 3, 191–198.
Downs, C.A., Mueller, E., Phillips, S., Fauth, J.E., Woodley, C.M., 2000. A molecular biomarker system for assessing the health of coral (*Montastraea faveolata*) during heat stress. Mar. Biotechnol. 2, 533–544.
Downs, C., Fauth, J.E., Halas, J.C., Dustan, P., Bemiss, J., Woodley, C.M., 2002. Oxidative stress and seasonal coral bleaching. Free Radic. Biol. Med. 33, 533–543.
Dunn, S.R., Thomason, J.C., Le Tissier, M.D., Bythell, J.C., 2004. Heat stress induces different forms of cell death in sea anemones and their endosymbiotic algae depending on temperature and duration. Cell Death Differ. 11, 1213–1222.
Duxbury, C.L., Dixon, D.G., Greenberg, B.M., 1997. Effects of simulated solar radiation on the bioaccumulation of polycyclic aromatic hydrocarbons by the duckweed *Lemna gibba*. Environ. Toxicol. Chem. 16, 1739–1748.
Foyer, C.H., Noctor, G., 2005. Redox homeostasis and antioxidant signaling: a metabolic interface between stress perception and physiological responses. Plant Cell 17, 1866–1875.
Grasso, L.C., Negri, A.P., Foret, S., Saint, R., Hayward, D.C., Miller, D.J., Ball, E.E., 2011. The biology of coral metamorphosis: molecular responses of larvae to inducers of settlement and metamorphosis. Dev. Biol. 353, 411–419.
Grundy, M.M., Ratcliffe, N.A., Moore, M.N., 1996. Immune inhibition in marine mussels by polycyclic aromatic hydrocarbons. Mar. Environ. Res. 42, 187–190.
Guzman, H.M., Burns, K.A., Jackson, J.B.C., 1994. Injury, regeneration and growth of Caribbean reef corals after a major oil spill in Panama. Mar. Ecol. Prog. Ser. 105, 231–241.
Hader, D.P., Williamson, C.E., Wangberg, S.A., Rautio, M., Rose, K.C., Gao, K.S., Helbling, E.W., Sinha, R.P., Worrest, R., 2015. Effects of UV radiation on aquatic ecosystems and interactions with other environmental factors. Photochem. Photobiol. Sci. 14, 108–126.
Hartmann, A.C., Sandin, S.A., Chamberland, V.F., Marhaver, K.L., de Goeij, J.M., Vermeij, M.J.A., 2015. Crude oil contamination interrupts settlement of coral larvae after direct exposure ends. Mar. Ecol. Prog. Ser. 536, 163–173.
Hartwell, L.H., Kastan, M.B., 1994. Cell cycle control and cancer. Science 266, 1821–1828.
Helton, E.S., Chen, X., 2007. p53 modulation of the DNA damage response. J. Cell. Biochem. 100, 883–896.
Heyward, A.J., Negri, A.P., 1999. Natural inducers for coral larval metamorphosis. Coral Reefs 18, 273–279.
Higuchi, T., Fujimura, H., Arakaki, T., Oomori, T., 2008. Activities of antioxidant enzymes (SOD and CAT) in the coral *Galaxea fascicularis* against increased hydrogen

peroxide concentrations in seawater. Proceeding of the 11th International Coral Reef Symposium.

Hughes, T.P., Baird, A.H., Bellwood, D.R., Card, M., Connolly, S.R., Folke, C., Grosberg, R., Hoegh-Guldberg, O., Jackson, J.B., Kleypas, J., Lough, J.M., Marshall, P., Nystrom, M., Palumbi, S.R., Pandolfi, J.M., Rosen, B., Roughgarden, J., 2003. Climate change, human impacts, and the resilience of coral reefs. Science 301, 929–933.

Hughes, T.P., Graham, N.A., Jackson, J.B., Mumby, P.J., Steneck, R.S., 2010. Rising to the challenge of sustaining coral reef resilience. Trends Ecol. Evol. 25, 633–642.

Hughes, T.P., Kerry, J.T., Álvarez-Noriega, M., Álvarez-Romero, J.G., Anderson, K.D., Baird, A.H., Babcock, R.C., Beger, M., Bellwood, D.R., Berkelmans, R., 2017. Global warming and recurrent mass bleaching of corals. Nature 543, 373–377.

Hutchins, C.M., Simon, D.F., Zerges, W., Wilkinson, K.J., 2010. Transcriptomic signatures in *Chlamydomonas reinhardtii* as Cd biomarkers in metal mixtures. Aquat. Toxicol. 100, 120–127.

Hwang, D.S., Lee, J.S., Rhee, J.S., Han, J., Lee, Y.M., Kim, I.C., Park, G.S., Lee, J., Lee, J.S., 2010. Modulation of p53 gene expression in the intertidal copepod *Tigriopus japonicus* exposed to alkylphenols. Mar. Environ. Res. 69, 77–80.

Jones, R., Ricardo, G.F., Negri, A.P., 2015. Effects of sediments on the reproductive cycle of corals. Mar. Pollut. Bull. 100, 13–33.

Kruse, J.P., Gu, W., 2009. Modes of p53 regulation. Cell 137, 609–622.

Krylov, S.N., Huang, X.D., Zeiler, L.F., Dixon, D.G., Greenberg, B.M., 1997. Mechanistic quantitative structure-activity relationship model for the photoinduced toxicity of polycyclic aromatic hydrocarbons. 1. Physical model based on chemical kinetics in a two-compartment system. Environ. Toxicol. Chem. 16, 2283–2295.

Kushmaro, A., Henning, G., Hofmann, D., Benayahu, Y., 1997. Metamorphosis of *Heteroxenia fuscescens* planulae (Cnidaria: Octocorallia) is inhibited by crude oil: a novel short term toxicity bioassay. Mar. Environ. Res. 43, 295–302.

Lee, H.J., Villaume, J., Cullen, D.C., Kim, B.C., Gu, M.B., 2003. Monitoring and classification of PAH toxicity using an immobilized bioluminescent bacteria. Biosens. Bioelectron. 18, 571–577.

Lesser, M.P., Farrell, J.H., 2004. Exposure to solar radiation increases damage to both host tissues and algal symbionts of corals during thermal stress. Coral Reefs 23, 367–377.

Levy, O., Achituv, Y., Yacobi, Y.Z., Stambler, N., Dubinsky, Z., 2006. The impact of spectral composition and light periodicity on the activity of two antioxidant enzymes (SOD and CAT) in the coral *Favia favus*. J. Exp. Mar. Biol. Ecol. 328, 35–46.

Linan-Cabello, M.A., Flores-Ramirez, L.A., Cobo-Diaz, J.F., Zenteno-Savin, T., Olguin-Monroy, N.O., Olivos-Ortiz, A., Tintos-Gomez, A., 2010. Response to short term ultraviolet stress in the reef-building coral *Pocillopora capitata* (Anthozoa: Scleractinia). Rev. Biol. Trop. 58, 103–118.

Livak, K.J., Schmittgen, T.D., 2001. Analysis of relative gene expression data using real-time quantitative PCR and the 2-DD CT method. Methods 25, 402–408.

Lyons, B.P., Pascoe, C.K., McFadzen, I.R., 2002. Phototoxicity of pyrene and benzo[a]pyrene to embryo-larval stages of the Pacific oyster *Crassostrea gigas*. Mar. Environ. Res. 54, 627–631.

McGrath, J.A., Di Toro, D.M., 2009. Validation of the target lipid model for toxicity assessment of residual petroleum constituents: monocyclic and polycyclic aromatic hydrocarbons. Environ. Toxicol. Chem. 28, 1130–1148.

Michiels, C., Raes, M., Toussaint, O., Remacle, J., 1994. Importance of Se-glutathione peroxidase, catalase, and Cu/Zn-SOD for cell survival against oxidative stress. Free Radic. Biol. Med. 17, 235–248.

Mittler, R., 2002. Oxidative stress, antioxidants and stress tolerance. Trends Plant Sci. 7, 405–410.

Negri, A.P., Heyward, A.J., 2000. Inhibition of fertilization and larval metamorphosis of the coral *Acropora millepora* (Ehrenberg, 1834) by petroleum products. Mar. Pollut. Bull. 41, 420–427.

Negri, A.P., Brinkman, D.L., Flores, F., Botte, E.S., Jones, R.J., Webster, N.S., 2016. Acute ecotoxicology of natural oil and gas condensate to coral reef larvae. Sci. Rep. 6, 21153.

Nii, C.M., Muscatine, L., 1997. Oxidative stress in the symbiotic sea anemone *Aiptasia pulchella* (Carlgren, 1943): contribution of the animal to superoxide ion production at elevated temperature. Biol. Bull. 192, 444–456.

Nordborg, F.M., Flores, F., Brinkman, D.L., Agusti, S., Negri, A.P., under review. Phototoxic effects of two common marine fuels on the settlement success of the coral *Acropora tenuis*. Nat. Sci. Rep.

Obermüller, B., Karsten, U., Abele, D., 2005. Response of oxidative stress parameters and sunscreening compounds in Arctic amphipods during experimental exposure to maximal natural UVB radiation. J. Exp. Mar. Biol. Ecol. 323, 100–117.

PGM-Environment, 2012. Great Barrier Reef Shipping: Review of Environmental Implications. PGM-Environment, Safety Bay, Western Australia p. 156.

Palmer, C.V., Modi, C.K., Mydlarz, L.D., 2009. Coral fluorescent proteins as antioxidants. PLoS One 4, e7298.

Pandolfi, J.M., Bradbury, R.H., Sala, E., Hughes, T.P., Bjorndal, K.A., Cooke, R.G., McArdle, D., McClenachan, L., Newman, M.J., Paredes, G., Warner, R.R., Jackson, J.B., 2003. Global trajectories of the long-term decline of coral reef ecosystems. Science 301, 955–958.

Pandolfi, J.M., Connolly, S.R., Marshall, D.J., Cohen, A.L., 2011. Projecting coral reef futures under global warming and ocean acidification. Science 333, 418–422.

Peachey, R.L., Crosby, D.G., 1996. Phototoxicity in tropical reef animals. Mar. Environ.

Res. 42, 359–362.

Pelletier, M.C., Burgess, R.M., Ho, K.T., Kuhn, A., McKinney, R.A., Ryba, S.A., 1997. Phototoxicity of individual polycyclic aromatic hydrocarbons and petroleum to marine invertebrate larvae and juveniles. Environ. Toxicol. Chem. 16, 2190–2199.

Ramos, R., Garcia, E., 2007. Induction of mixed-function oxygenase system and anti-oxidant enzymes in the coral *Montastraea faveolata* on acute exposure to benzo(a) pyrene. Comp. Biochem. Physiol. C: Toxicol. Pharmacol. 144, 348–355.

Redman, A.D., Parkerton, T.F., McGrath, J.A., Di Toro, D.M., 2012. PETROTOX: an aquatic toxicity model for petroleum substances. Environ. Toxicol. Chem. 31, 2498–2506.

Rhee, J.-S., Kim, B.-M., Kim, R.-O., Seo, J.S., Kim, I.-C., Lee, Y.-M., Lee, J.-S., 2013. Co-expression of antioxidant enzymes with expression of p53, DNA repair, and heat shock protein genes in the gamma ray-irradiated hermaphroditic fish *Kryptolebias marmoratus* larvae. Aquat. Toxicol. 140, 58–67.

Richier, S., Sabourault, C., Courtiade, J., Zucchini, N., Allemand, D., Furla, P., 2006. Oxidative stress and apoptotic events during thermal stress in the symbiotic sea anemone, *Anemonia viridis*. FEBS J. 273, 4186–4198.

Rinkevich, B., Loya, Y., 1977. Harmful effects of chronic oil pollution on a Red Sea scleractinian coral population. In: Proceedings of the Third International Coral Reef Symposium. Miami, Florida. pp. 585–591.

Rinkevich, B., Loya, Y., 1979. Laboratory experiments on the effects of crude oil on the Red Sea coral *Stylophora pistillata*. Mar. Pollut. Bull. 10, 328–330.

Rodriguez-Lanetty, M., Harii, S., Hoegh-Guldberg, O., 2009. Early molecular responses of coral larvae to hyperthermal stress. Mol. Ecol. 18, 5101–5114.

Salih, A., Larkum, A., Cox, G., Kuhl, M., Hoegh-Guldberg, O., 2000. Fluorescent pigments in corals are photoprotective. Nature 408, 850–853.

Sandrini, J.Z., Trindade, G.S., Nery, L.E., Marins, L.F., 2009. Time-course expression of DNA repair-related genes in hepatocytes of zebrafish (*Danio rerio*) after UV-B exposure. Photochem. Photobiol. 85, 220–226.

Shackelford, R.E., Kaufmann, W.K., Paules, R.S., 1999. Cell cycle control, checkpoint mechanisms, and genotoxic stress. Environ. Health Perspect. 107 (Suppl. 1), 5–24.

Shaw, M., Negri, A., Fabricius, K., Mueller, J.F., 2009. Predicting water toxicity: pairing passive sampling with bioassays on the Great Barrier Reef. Aquat. Toxicol. 95, 108–116.

Shick, J.M., Lesser, M.P., Dunlap, W.C., Stochaj, W.R., Chalker, B.E., Won, J.W., 1995. Depth-dependent responses to solar ultraviolet-radiation and oxidative stress in the zooxanthellate coral Acropora-microphthalma. Mar. Biol. 122, 41–51.

Smith-Keune, C., Dove, S., 2008. Gene expression of a green fluorescent protein homolog as a host-specific biomarker of heat stress within a reef-building coral. Mar. Biotechnol. 10, 166–180.

Soriano-Santiago, O.S., Linan-Cabello, M.A., Delgadillo-Nuno, M.A., Ortega-Ortiz, C., Cuevas-Venegas, S., 2013. Physiological responses to oxidative stress associated with pH variations in host tissue and zooxanthellae of hermatypic coral *Pocillopora capitata*. Mar. Freshw. Behav. Physiol. 46, 275–286.

Souter, P., Bay, L.K., Andreakis, N., Csaszar, N., Seneca, F.O., van Oppen, M.J., 2011. A multilocus, temperature stress-related gene expression profile assay in *Acropora millepora*, a dominant reef-building coral. Mol. Ecol. Resour. 11, 328–334.

Tarrant, A.M., Reitzel, A.M., Kwok, C.K., Jenny, M.J., 2014. Activation of the cnidarian oxidative stress response by ultraviolet radiation, polycyclic aromatic hydrocarbons and crude oil. J. Exp. Biol. 217, 1444–1453.

Teal, J.M., Howarth, R.W., 1984. Oil-spill studies – a review of ecological effects. Environ. Manage. 8, 27–43.

Tebben, J., Motti, C.A., Siboni, N., Tapiolas, D.M., Negri, A.P., Schupp, P.J., Kitamura, M., Hatta, M., Steinberg, P.D., Harder, T., 2015. Chemical mediation of coral larval settlement by crustose coralline algae. Sci. Rep. 5, 10803.

Turner, N.R., Renegar, D.A., 2017. Petroleum hydrocarbon toxicity to corals: a review. Mar. Pollut. Bull. 119, 1–16.

Villanueva, R.D., Yap, H.T., Montano, M.N., 2011. Reproductive effects of the water-accommodated fraction of a natural gas condensate in the Indo-Pacific reef-building coral *Pocillopora damicornis*. Ecotoxicol. Environ. Saf. 74, 2268–2274.

Voolstra, C.R., Schnetzer, J., Peshkin, L., Randall, C.J., Szmant, A.M., Medina, M., 2009. Effects of temperature on gene expression in embryos of the coral *Montastraea faveolata*. BMC Genomics 10, 627.

Wang, Y., Chen, J.W., Li, F., Qin, H., Qiao, X.L., Hao, C., 2009. Modeling photoinduced toxicity of PAHs based on DFT-calculated descriptors. Chemosphere 76, 999–1005.

Wilkinson, C.R., 1999. Global and local threats to coral reef functioning and existence: review and predictions. Mar. Freshw. Res. 50, 867–878.

Willis, A.M., Oris, J.T., 2014. Acute photo-induced toxicity and toxicokinetics of single compounds and mixtures of polycyclic aromatic hydrocarbons in zebrafish. Environ. Toxicol. Chem. 33, 2028–2037.

Yuyama, I., Harii, S., Hidaka, M., 2012a. Algal symbiont type affects gene expression in juveniles of the coral *Acropora tenuis* exposed to thermal stress. Mar. Environ. Res. 76, 41–47.

Yuyama, I., Ito, Y., Watanabe, T., Hidaka, M., Suzuki, Y., Nishida, M., 2012b. Differential gene expression in juvenile polyps of the coral *Acropora tenuis* exposed to thermal and chemical stresses. J. Exp. Mar. Biol. Ecol. 430, 17–24.

Zbigniew, T., Wojciech, P., 2006. Individual and combined effect of anthracene, cadmium, and chloridazone on growth and activity of SOD izoformes in three *Scenedesmus* species. Ecotoxicol. Environ. Saf. 65, 323–331.